IOPscience iopscience.iop.org

Home Search Collections Journals About Contact us My IOPscience

On the non-equivalence of observables in phase-space reconstructions from recorded time series

This article has been downloaded from IOPscience. Please scroll down to see the full text article.

1998 J. Phys. A: Math. Gen. 31 7913

(http://iopscience.iop.org/0305-4470/31/39/008)

View the table of contents for this issue, or go to the journal homepage for more

Download details:
IP Address: 171.66.16.102
The article was downloaded on 02/06/2010 at 07:13

Please note that terms and conditions apply.

J. Phys. A: Math. Gen. **31** (1998) 7913–7927. Printed in the UK PII: S0305-4470(98)93312-1

On the non-equivalence of observables in phase-space reconstructions from recorded time series

C Letellier†§, J Maquet†, L Le Sceller†, G Gouesbet† and L A Aguirre‡

† LESP-UMR 6614-CORIA, Université et INSA de Rouen, Place Emile Blondel, 76131 Mont Saint-Aignan Cedex, France

‡ Centro de Pesquisa e Desenvolvimento em Engenharia Elétrica, Departamento de Enga. Eletronica, Universidade Federal de Minas Gerais, Av. Antônio Carlos 6627, 31.270-901 Belo Horizonte, MG, Brazil

Received 14 April 1998, in final form 26 June 1998

Abstract. In practical problems of phase-space reconstruction, it is usually the case that the reconstruction is much easier using a particular recorded scalar variable. This seems to contradict the general belief that all variables of a dynamical system are equivalent in phase-space reconstruction problems. This paper will argue that, in many cases, the choice of a particular scalar time series from which to reconstruct the original dynamics could be critical. It is argued that different dynamical variables do not provide the same level of information (observability) of the underlying dynamics and, as a consequence, the quality of a global reconstruction critically depends on the recorded variable. Examples in which the choice of observables is critical are discussed and the level of information contained in a given variable is quantified in the case where the original system is known. A clear example of such a situation arises in the Rössler system for which the performance of a global vector field reconstruction technique is investigated using time series of variables x, y or z, taken one at a time.

1. Introduction

The aim of a phase-space reconstruction is to generate a multidimensional phase space from a recorded scalar time series. It is a prerequisite step for analysing the behaviour of a dynamical system which is only known from a single (scalar) time series. A pioneering paper by Packard *et al* [1] points out two ways of reconstructing a state space, namely by using time delay or time derivative coordinates. Another kind of coordinates, namely principal components [2], may also be used. Gibson *et al* [3] demonstrated that the relationship between delays, derivatives and principal components consists of a rotation and a rescaling. Consequently, from Gibson's point of view, statements about the nature of the equivalence between the original and the reconstructed phase portraits would not depend on the coordinate system.

Furthermore, there is also a great deal of interest in reconstructing a set of differential equations from a single variable time series ([4–12] among others). According to Takens' theorem [13], it is always possible to construct an embedding of a time series in a phase space in the absence of noise. To ensure, with probability one, that a reconstruction is an embedding, i.e. that there exists a diffeomorphism from the original phase space to the embedding space, the embedding dimension has to be $d_E \geqslant 2D_H+1$ where D_H ideally refers

§ E-mail address: letellie@coria.fr

0305-4470/98/397913+15$19.50 © 1998 IOP Publishing Ltd

to the Hausdorff–Besicovitch dimension of the attractor studied. If the above criterion is not satisfied, the existence of a diffeomorphism is not ensured but nevertheless remains possible. Indeed, Sauer *et al* [14] demonstrated that, in principle, a reconstructed phase space with a dimension equal to the first integer greater than the correlation dimension could be sufficient to completely describe the dynamics of the system studied. This statement has also been confirmed by computing an embedding dimension with the aid of a false nearest-neighbours method [15–17].

Unfortunately, it is also established that a time series, even infinite and noise-free, may fail to contain all relevant information, meaning that the measurement function introduced in Takens' theorem is not well defined. This fact also means that the ability to observe the state of a system may depend on the recorded variable, as exemplified in [18–20]. Obvious cases are provided by equivariant systems for which two kinds of time series may appear (i) equivariant time series containing information about symmetry properties and (ii) invariant time series without any information on symmetry properties, such as for the well known Lorenz system (see [18, 19]). More generally, it is not ensured that all dynamical variables of a given system are equivalent to obtain reconstructed phase spaces or reconstructed models. In this paper, such a statement is exemplified in the case of the Rössler system for which global vector field reconstructions in a 3D space, from the z variable, always failed up to now [8]. Variable z of the Rössler system therefore exhibits a somewhat pathological character. This is confirmed, from another point of view, by Kugiumtzis [20] who states that the z variable hardly allows one to identify the orbital periods while they are easily identified from the other variables. Also, the correlation dimension is significantly underestimated when using variable z while it is correctly estimated from x measurements [20].

This paper intends to discuss and show that the ability of reconstructing the phase space of a system may depend critically on the observable being used. Such a dependence will be quantified by using an observability index in the case of well known systems. Our goal here is to clearly exhibit that all dynamical variables of a given system are not equivalent when their time evolutions are used as scalar time series to investigate the underlying dynamics. An explicit example will be discussed in the case of the variables of the Rössler system for which the relative observability among the variables of this system is quantified by using the observability index. It will be shown that it is more difficult to obtain a model from the z variable than from the others as suggested by the observability index.

The paper is organized as follows. Section 2 briefly describes the global vector field reconstruction technique and points out the problem arising when reconstructing a model from the variable z of the Rössler system. Section 3 uses an observability index to compare the relative observability of the x, y and z variables of the Rössler system. The results in this section are in good accord with widespread practice of reconstructing attractors from such a system. Section 4 exhibits the difficulties encountered in reconstructing a model from the variable z of the Rössler system. Section 5 is a conclusion.

2. Global vector field reconstruction

2.1. Theoretical background

Let us consider a time-continuous dynamical system described by a set of ordinary differential equations:

$$\dot{\boldsymbol{x}} = \boldsymbol{f}(\boldsymbol{x}; \mu) \tag{1}$$

in which $\boldsymbol{x}(t) \in \mathbb{R}^n$ is a vector valued function depending on a parameter t called the time and $\boldsymbol{f}$, the so-called vector field, is an n-component smooth function generating a flow ϕ_t. Also, $\mu \in \mathbb{R}^p$ is the parameter vector with p components, assumed to be constant in this paper. The system (1) is called the *original system*. The original system may be written as

$$\begin{aligned} \dot{x} &= f_1(x, y, z) \\ \dot{y} &= f_2(x, y, z) \\ \dot{z} &= f_3(x, y, z). \end{aligned} \tag{2}$$

It is now assumed that the observer numerically records a scalar time series. By convention, in this section, the observable is taken to be $X = x$.

The aim is then to reconstruct a vector field equivalent (we will later discuss in which sense) to the original system under the form of a reconstructed system made of the observable and of its derivatives according to

$$\begin{aligned} \dot{X}_1 &= X_2 \\ \dot{X}_2 &= X_3 \\ &\vdots \\ \dot{X}_{d_E} &= F(X_1, X_2, \ldots, X_{d_E}) \end{aligned} \tag{3}$$

where d_E is the embedding dimension and F depends on d_E variables which are the successive derivatives of x

$$\begin{aligned} X_1 &= x \\ X_2 &= \dot{x} \\ X_3 &= \ddot{x} \\ &\vdots \end{aligned} \tag{4}$$

F is called the standard function and can be estimated by using a multivariate polynomial basis on nets [8] which may be built by means of a Gram–Schmidt orthogonalization procedure [21]. The algorithm requires the definition of reconstruction parameters which are (i) d_E, the embedding dimension, (ii) N_q, the number of vectors $(X_{1,i}, X_{2,i}, \ldots, X_{d_E,i})$ $(i \in [1, N_q])$ on the net, with i a time index, (iii) Δt, the time step between two successive such vectors which may be expressed as the number of vectors, N_s, sampled per pseudo-period, (iv) N_p, the number of retained multivariate polynomials and (v) τ_w, the window length on which the derivatives are computed by using a sixth-degree interpolated polynomial. These interpolated polynomials are centred at each point by using the six nearest neighbours. Derivatives are then obtained by analytically differentiating such polynomials. The estimated standard function, denoted $\tilde{F}$, then has the form

$$\tilde{F}(X_1, X_2, \ldots, X_{d_E}) = \sum_{p=1}^{N_p} K_p \; \Xi^p \tag{5}$$

where Ξ^p is a multivariate monomial

$$\Xi^p = X_1^{n_1} X_2^{n_2} \ldots X_{d_E}^{n_{d_E}} \tag{6}$$

in which the integers p are related to n_{d_E}-tuplets $(n_1, n_2, \ldots, n_{d_E})$ by a bijective relationship discussed in [8]. Reconstruction parameters are determined with the aid of an error function described in [22]. Large sets of reconstruction parameters can, in practice, be related to an easy reconstruction.

2.2. Equivalences for the Rössler system

The original system is now assumed to be the Rössler system

$$\begin{aligned} \dot{x} &= -y - z \\ \dot{y} &= x + ay \\ \dot{z} &= b + z(x - c) \end{aligned} \tag{7}$$

where $a = 0.398$, $b = 2.0$ and $c = 4.0$ are the control parameters. The minimal embedding dimension d_E is therefore equal to 3. In this case, a transformation map Φ_i expressing the derivative coordinates (X, Y, Z) versus the original coordinates (x, y, z) may be obtained according to

$$\Phi_i \equiv \begin{cases} X = x_i \\ Y = \dot{x}_i = f(x, y, z) \\ Z = \dot{x}\dfrac{\partial f}{\partial x} + \dot{y}\dfrac{\partial f}{\partial y} + \dot{z}\dfrac{\partial f}{\partial z} \end{cases} \tag{8}$$

where the subscript i depends on the x_i time series used ($x_i = x$, y or z). Therefore, $\Phi_i : \mathbb{R}^3 \to \mathbb{R}^3$ is a well-defined map without any singularity since the original vector field $\boldsymbol{f}$ is smooth. Let us now focus on the original attractor A_{OS} defined by $(x(t), y(t), z(t))$ in the limit $t \to \infty$. The reconstructed attractor A_{RS} generated by integrating the reconstructed model may be obtained from A_{OS} by using Φ_i. Also, as the original system is known, algebraic manipulations allow one to find the exact expression of the standard function $F(X, Y, Z)$, for i chosen.

Let us consider a transformation map $\Phi = \Phi_i$, ($i = x$, y or z). We are then interested to know how an original attractor A_{OS} is mapped by such a transformation Φ and the nature of the equivalence between A_{OS} and A_{RS}. Algebraic considerations on Φ determine whether the transformation is an embedding, an immersion or worst an immersion that fails to be one-to-one [14].

When Φ defines a diffeomorphism, the reconstructed attractor is subject to the most severe constraints. Such a diffeomorphic equivalence between original and reconstructed attractors may be established by relying on the local properties of the transformation Φ. When $d_E = n$, this is achieved following the inverse function theorem [23, 24] which states that the transformation Φ is a diffeomorphism iff its Jacobian matrix $D\Phi$ is nowhere singular. *Such a diffeomorphism indeed exists between the original attractor A_{OS} and the attractor reconstructed from the y variable of the Rössler system.* Conversely, x and z variables provide transformations Φ_x and Φ_z with Jacobian matrices that vanish on a set of Lebesgue measure zero. These facts may be readily checked by the reader with a small amount of algebra. Φ_x and Φ_z therefore define almost everywhere a diffeomorphism. Consequently, the y variable is the best observable to reconstruct the dynamics of the Rössler system from a scalar time series.

It must be noted, however, that a transformation Φ can in practice be considered as an embedding even if it fails to pass the analytical test in some subset of the original phase space. Indeed, we are only interested in the properties of the restriction of the map to the strange attractor, which is a subset of volume zero. Therefore, singularities located outside of the strange attractor could possibly not matter when a global vector field reconstruction is the issue considered. However, inner singularities can greatly affect the quality of a reconstructed model as it be shown using the z variable of the Rössler system.

2.3. Influence of singularities

The original system is the Rössler system whose phase space is spanned by the original coordinates (x, y, z). The reconstructed attractors which are spanned by derivative coordinates (X, Y, Z) are denoted A_x, A_y and A_z where the subscript is associated with the observable used. Transformations Φ_x, Φ_y and Φ_z which map the original coordinates (x, y, z) to the derivative coordinates (X, Y, Z) may be easily obtained by using relation (8). In any case, X will be associated with the scalar time series from which the attractor is reconstructed.

When the transformation Φ defines a diffeomorphism, both Φ and Φ^{-1} are everywhere defined and, consequently, do not involve any singularity, i.e. in particular do not involve any rational function. To a polynomial vector field then corresponds a polynomial standard function. In the case of the Rössler system, this happens when y is the observable. Indeed, the standard function F_y is a polynomial [8, 25]:

$$F_y = -b - cX + (ac - 1)Y + (a - c)Z - aX^2 + (a^2 + 1)XY - aXZ - aY^2 + YZ. \quad (9)$$

The polynomial structure of this exact standard function F_y matches the polynomial structure of the estimated standard function $\tilde{F}_y$ which is imposed by the reconstruction algorithm. As a consequence, reconstructions with the variable y are found to be exceptionally robust, i.e. they are successful for a very large set of reconstruction parameters. The variable y is therefore a very good observable for reconstructing the Rössler system.

Conversely, Φ_x and Φ_z do not define a diffeomorphism everywhere but only almost everywhere. Indeed, the Jacobian matrices become similar on sets of Lebesgue measure zero, namely $x = a + c$ for Φ_x and $z^2 = 0$ for Φ_z [25]. Accordingly, the maps Φ^{-1} exhibit singularities as shown below:

$$\Phi_x^{-1} \equiv \begin{cases} x = X \\ y = -\dfrac{b + X + Z + Y(c - X)}{a + c - X} \\ z = \dfrac{b + X - aY + Z}{a + c - X} \end{cases} \qquad \text{with} \quad \begin{cases} X = x \\ Y = \dot{x} \\ Z = \ddot{x} \end{cases} \quad (10)$$

and

$$\Phi_z^{-1} \equiv \begin{cases} x = c + \dfrac{Y - b}{X} \\ y = -X - \dfrac{Z}{X} + \dfrac{Y(Y - b)}{X^2} \\ z = X \end{cases} \qquad \text{with} \quad \begin{cases} X = z \\ Y = \dot{z} \\ Z = \ddot{z}. \end{cases} \quad (11)$$

The standard function F_x reads as

$$F_x = ab - cX + X^2 - aXY + XZ + acY + (a - c)Z - \frac{(a + c + Z - aY + b)Y}{a + c - X} \quad (12)$$

and presents a first-order singularity while the standard function F_z presents a second-order singularity:

$$F_z = b - cX - Y + aZ + aX^2 - XY + \frac{(ab + 3Z)Y - aY^2 - bZ}{X} + \frac{2bY^2 - 2Y^3}{X^2}. \quad (13)$$

In such cases, the reconstructed standard functions do not possess the same mathematical structure as the exact standard function but, due to the Weierstrass approximation theorem [26], the reconstructions may still be successful depending on how the reconstructed function will be close to the original function. However, we expect that successful reconstructions

will become more difficult when the order of the singularity increases. We therefore propose a first classification of the dynamical variables of the Rössler system according to the order of the singularity involved in the standard function, associated with greater or lesser facility to reconstruct the phase space. Loosely speaking, this can be related to the amount of information observed using such a variable. We then obtain $y \triangleright x \triangleright z$ where $\triangleright$ means 'provides a better observability of the underlying dynamics than'. This order ranges from the easiest case (diffeomorphism, no singularity, i.e. zeroth-order singularity) to the most difficult case of the variable z. Indeed, the variable x did allow us to obtain satisfactory reconstructions [8] while, when using variable z, the global vector field reconstruction technique always failed until now. It is one of the by-products of this paper to reconstruct the Rössler system using this variable, as detailed in section 4.

3. Observability Test

The concept of observability in linear system theory is standard and well defined [27]. Consider the system

$$\begin{cases} \dot{x} = Ax + Bu \\ \dot{y} = Cx \end{cases} \tag{14}$$

where $x \in \mathbb{R}^n$ is the state vector, $y \in \mathbb{R}^r$ is the measurement vector, $u \in \mathbb{R}^p$ is the input vector and $\{A, B, C\}$ are constant matrices. Thus the system (14) is said to be state observable at time t_f if the initial state $x(0)$ can be uniquely determined from knowledge of a finite time history of the input $u(\tau)$ and output $y(\tau)$, $0 \leqslant \tau \leqslant t_f$ [28]. It should be noted that the definition is still valid for autonomous systems, that is, for $u(\tau) = 0$.

One way of testing if the system (14) is observable is to define the *observability matrix*

$$Q = \begin{bmatrix} C \\ CA \\ CA^2 \\ \vdots \\ CA^{n-r} \end{bmatrix}. \tag{15}$$

The system (14) is therefore state observable if matrix Q is full rank, that is if $\mathrm{rank}(Q) = n$. This definition is a 'yes' or 'no' measurement of observability, i.e. the system is either observable or not. In practice, however, a system may gradually become unobservable as a parameter is varied. Thus it is useful to define the degree of observability as

$$\delta_{\mathrm{o}} = \frac{|\lambda_{\min}(QQ^T)|}{|\lambda_{\max}(QQ^T)|} \tag{16}$$

where $(\cdot)^T$ indicates the transpose, $\lambda_{\min}$ and $\lambda_{\max}$ are the minimum and maximum eigenvalues. Thus $0 \leqslant \delta_{\mathrm{o}} \leqslant 1$, and the lower bound is reached when the system is unobservable. Note that the index (16) is a type of condition number of the observability matrix.

In this section the observability index is used to quantify the relative observability of the Rössler system when observed from variables x, y and z. In order to do so, the Jacobian of the system is evaluated along trajectories on the attractor, observed from such variables. Thus in this case matrix A is the Jacobian of the Rössler system, $B = 0$ and three different situations for matrix C are considered, namely $C = [1\ 0\ 0]$, $C = [0\ 1\ 0]$ and $C = [0\ 0\ 1]$ indicating when the system is observed from x, y and z, respectively.

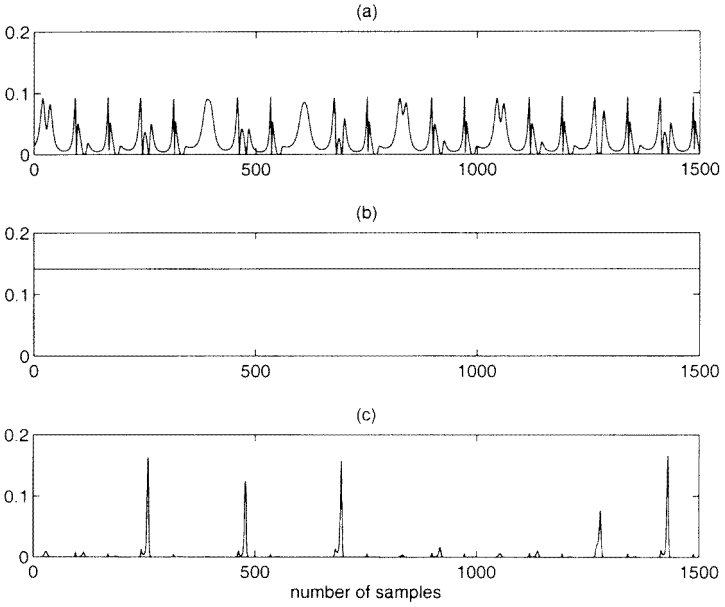

Figure 1. Observability index for the Rössler system along a trajectory with 1500 samples. (*a*) δ_{ox}, (*b*) δ_{oy}, and (*c*) δ_{oz}. The mean values are $\overline{\delta_{ox}} = 0.024$, $\overline{\delta_{oy}} = 0.141$ and $\overline{\delta_{oz}} = 0.003$.

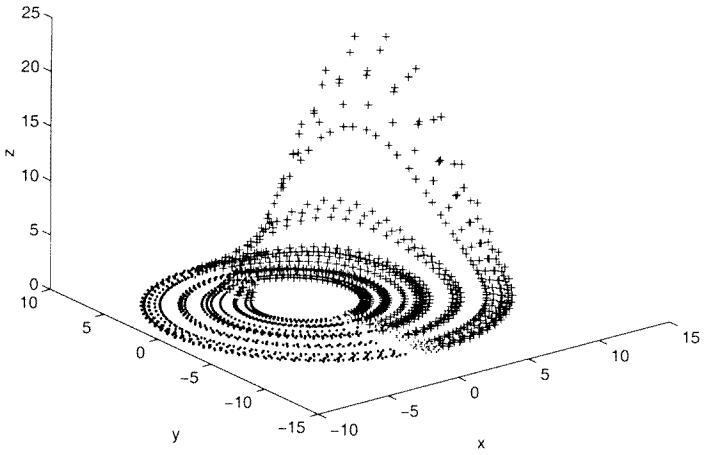

Figure 2. Rössler attractor. In this figure, two different symbols were used to plot the trajectories, depending on the relative degree of observability. At each point on the attractor, the observability index (16) was calculated for the case of the variable z. If the respective value was greater than a given threshold the point was indicated with a cross, otherwise it was indicated with a dot.

Figure 1 shows the observability index calculated for the Rössler system over 1500 samples of an orbit of the chaotic attractor observed from the three variables. The mean values are $\overline{\delta_{ox}} = 0.024$, $\overline{\delta_{oy}} = 0.141$ and $\overline{\delta_{oz}} = 0.003$. Both the plots and these average values are in perfect accord with the results presented in section 2.3. It is interesting to point out that the observability index calculated from the y variable is constant, that is, it

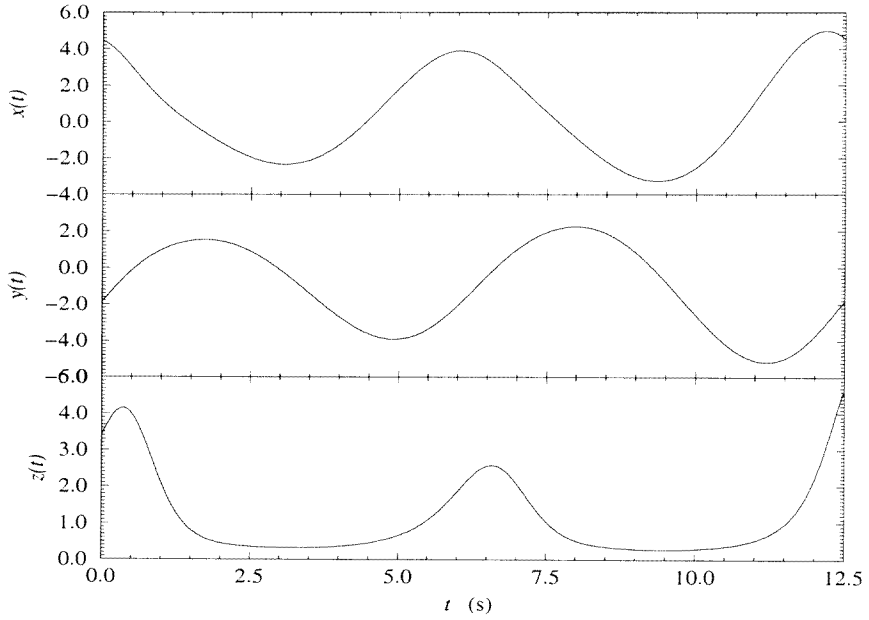

Figure 3. The dynamical variable z presents lethargies during which it contains a low rate of information on the time evolution of the other variables.

does not depend on where the system is in phase space. This is presumably a consequence of the existence of a diffeomorphism. On the other hand, δ_{ox} is quite oscillatory and δ_{oz} is negligible most of the time. The values of the observability index in these cases obviously depend on where the system is in phase space. For instance, the observability index (16) shown in figure 1 is displayed in figure 2 versus the location on the Rössler attractor for the case of the variable z. If δ_{oz} was greater than a certain threshold crosses were used in the plot otherwise dots were employed. This figure clearly shows that the Rössler attractor becomes more observable when it leaves the xy plane, i.e. when the evolution of the dynamics is approximately parallel to the z variable. The xy plane corresponds to the neighbourhood of the singularity $z = 0$ of the standard function F_z. We therefore conjecture that whenever the system comes close to a singularity (see section 2.3) the respective observability index decreases.

In closing this section, it is pointed out that the same procedure outlined here was performed for the Lorenz system. Once again, the results confirmed previous findings, namely that for such a system the z variable is the most adequate for phase-space reconstruction [8]. In fact, for the Lorenz system $\overline{\delta_{oz}}$ is one order of magnitude greater than $\overline{\delta_{oy}}$, the second largest observability index.

4. Reconstructing the Rössler system

The very low observability index of the z variable of the Rössler system may be understood by remarking that lethargies (long time with very small amplitude change) are observed on the z time series, even though the dynamical variables x and y present significant amplitude changes (figure 3). When working in a reconstructed 3D space, these lethargies induce the presence of segments close to tangency, i.e. close to situations where identical phase

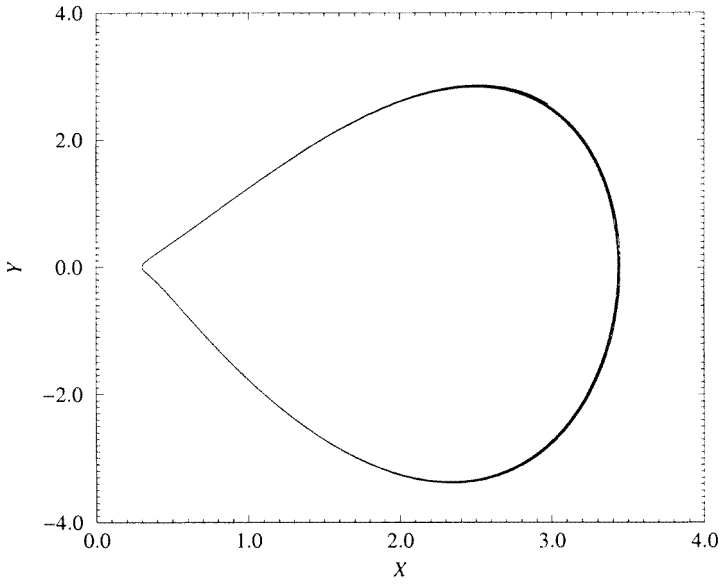

Figure 4. Reconstruction of a limit cycle instead of a chaotic attractor starting from the variable z of the Rössler system.

points would generate different futures, conflicting with causality. This phenomenon is amplified by sampling the time series both in time and in amplitude since some amount of information concerning the differential structure is then lost. Such quasi-tangencies cannot necessarily be resolved by working in a 3D phase space. The determinism principle is then in practice violated and, as a result, satisfactory reconstructed models cannot easily be obtained. Instead, depending on the reconstruction parameters, we find that the reconstructed models generate a limit cycle (figure 4) or are numerically unstable and diverge to infinity after a transient behaviour (figure 5). How the reconstruction fails (figures 4 and 5) makes much sense.

Since the dynamics cannot be successfully captured by a 3D model, we use Takens' theorem as a guide and ask whether a higher embedding dimension would allow one to obtain a satisfactory model. As a preliminary test, we then evaluate an estimation of the embedding dimension by using an adapted false nearest-neighbour technique [17]. We then find that an embedding dimension equal to 3 is satisfactory for the variables y and x (figure 6). For the variable z, however, figure 6 points out that an embedding dimension as large as 8 might be required. The results in figure 6 were computed with a rather small amount of data (10 000 points in the time series) and, in this example, the sampling of trajectories close to tangency blurs information in a way which is similar to additive noise. They therefore must be interpreted with some care and taken as indicative. They nevertheless suggest that a satisfactory model with variable z could be obtained by increasing the embedding dimension. Also, they suggest that such a large embedding dimension as $d_E \approx 8$ could be unnecessary since figure 6 exhibits some amount of saturation for $d_E \approx 4$. It is expected also that such an increase in d_E could be sufficient to smooth out the effect of the quasi-tangencies observed in a 3D space.

We therefore attempt a global vector field reconstruction in a 4D phase space. A successful reconstruction is then indeed obtained with the following values of the

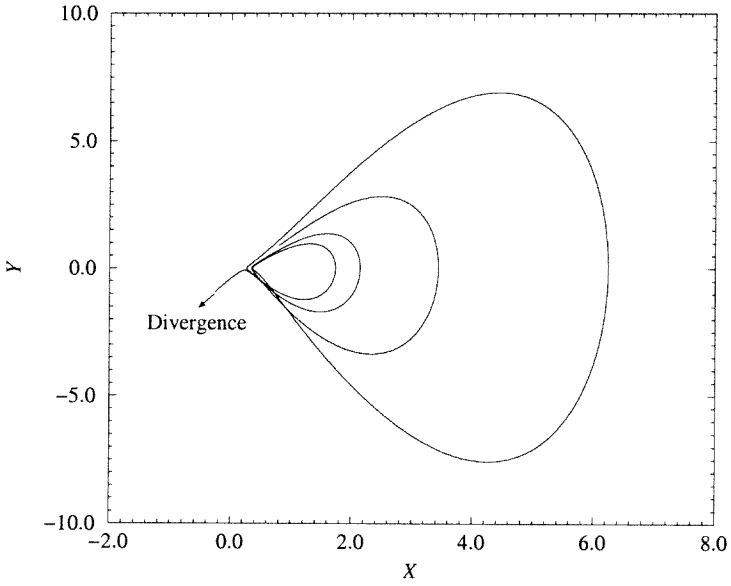

Figure 5. Reconstruction of a numerically unstable model starting from the dynamical variable z of the Rössler system. The trajectory is ejected to infinity from the vicinity of the origin associated to the pole of the approximated standard function.

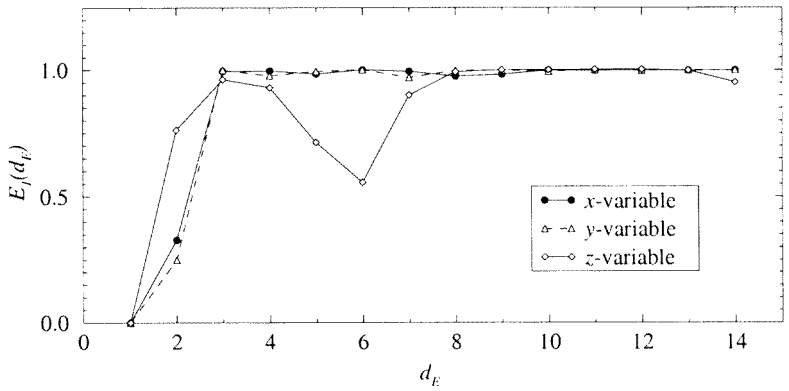

Figure 6. Embedding dimension of the reconstructed attractors computed by using an adapted false nearest-neighbour method. In this method, the ordinates saturate when the embedding dimension is large enough. Index $E_1(d_E)$ measures the relative change in the average distance between two neighbour points in R^{d_E} and their respective images in R^{d_E+1} when the embedding dimension is increased from d_E to $d_E + 1$.

reconstruction parameters:

$$\begin{aligned} d_E &= 4 \\ N_q &= 150 \\ N_s &= 14 \\ N_p &= 35 \end{aligned} \tag{17}$$

leading to the chaotic attractor displayed in figure 7. The coefficients K_p of the estimated

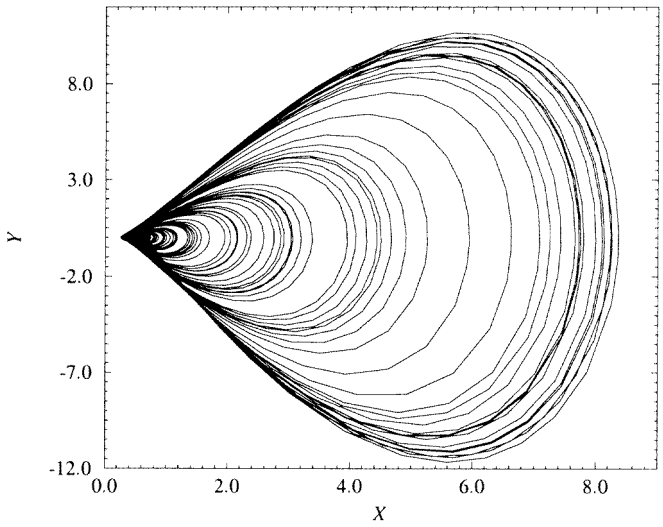

Figure 7. Plane projection of the attractor generated by integrating the four-variable reconstructed model.

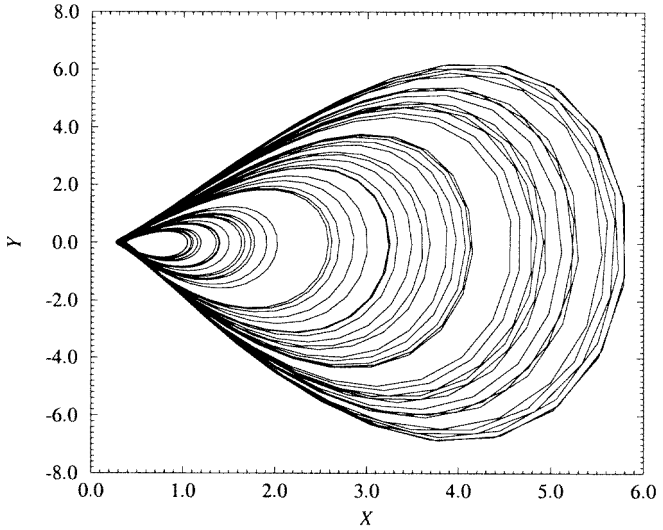

Figure 8. Plane projection of the attractor generated by applying the map Φ_z to the original attractor.

standard function $\tilde{F}_z$ are listed in table 1. This attractor compares fairly well with the attractor obtained by applying the map Φ_z to the original attractor (figure 8), in which

$$\Phi_z = \begin{cases} X = z \\ Y = c + \dfrac{Y - b}{X} \\ Z = -X - \dfrac{Z}{X} + \dfrac{Y(Y-b)}{X^2}. \end{cases} \tag{18}$$

The basic structure of both attractors is the same and slight differences in amplitude arise

Table 1. K_p coefficients of the approximated standard function $\tilde{F}_z$.

p	K_p	i	j	k	l
1	0.489 407 814 957 45	0	0	0	0
2	$-0.145\,639\,664\,263\,10 \cdot 10^{2}$	1	0	0	0
3	$0.139\,255\,049\,017\,02 \cdot 10^{2}$	0	1	0	0
4	$-0.635\,197\,165\,563\,23 \cdot 10^{1}$	0	0	1	0
5	$0.586\,960\,526\,882\,71 \cdot 10^{1}$	0	0	0	1
6	$0.148\,613\,068\,193\,55 \cdot 10^{3}$	2	0	0	0
7	0.531 670 076 508 45	1	1	0	0
8	$-0.432\,326\,112\,170\,02 \cdot 10^{2}$	1	0	1	0
9	$-0.422\,885\,224\,692\,21 \cdot 10^{2}$	1	0	0	1
10	$0.171\,734\,374\,763\,68 \cdot 10^{3}$	0	2	0	0
11	$0.788\,866\,514\,520\,96 \cdot 10^{2}$	0	1	1	0
12	$-0.810\,356\,308\,253\,23 \cdot 10^{1}$	0	1	0	1
13	$0.127\,851\,608\,885\,64 \cdot 10^{2}$	0	0	2	0
14	−0.104 919 989 280 33	0	0	1	1
15	$0.152\,837\,252\,970\,32 \cdot 10^{-1}$	0	0	0	2
16	$-0.229\,126\,919\,438\,01 \cdot 10^{3}$	3	0	0	0
17	$-0.715\,880\,744\,707\,95 \cdot 10^{2}$	2	1	0	0
18	$-0.548\,332\,996\,824\,38 \cdot 10^{2}$	2	0	1	0
19	−0.926 491 592 260 28	2	0	0	1
20	$0.141\,973\,897\,883\,40 \cdot 10^{2}$	1	2	0	0
21	$-0.846\,907\,146\,269\,83 \cdot 10^{1}$	1	1	1	0
22	−0.613 126 828 204 80	1	1	0	1
23	$-0.845\,155\,888\,763\,10 \cdot 10^{1}$	1	0	2	0
24	$-0.116\,514\,699\,050\,96 \cdot 10^{1}$	1	0	1	1
25	$-0.858\,101\,354\,152\,74 \cdot 10^{-1}$	1	0	0	2
26	$0.421\,871\,751\,410\,20 \cdot 10^{1}$	0	3	0	0
27	$0.121\,781\,905\,212\,47 \cdot 10^{2}$	0	2	1	0
28	$0.233\,228\,325\,370\,95 \cdot 10^{1}$	0	2	0	1
29	−0.659 674 148 554 91	0	1	2	0
30	0.467 071 843 045 66	0	1	1	1
31	0.106 571 853 493 62	0	1	0	2
32	−0.408 361 154 012 21	0	0	3	0
33	−0.145 437 760 421 84	0	0	2	1
34	$-0.862\,179\,781\,151\,60 \cdot 10^{-3}$	0	0	1	2
35	$-0.123\,550\,755\,401\,24 \cdot 10^{-3}$	0	0	0	3

from the fact that population of periodic orbits are slightly different as explained below.

We would now like to present an objective validation of the reconstructed model. When the dimension of the phase space is 3, our favourite method is the topological characterization based on knot theory [29, 30]. Unfortunately, in the present case where $d_E = 4$, no *stricto sensu* topological characterization is so far available. Nevertheless, because the fourth variable is essentially used to unfold the manifolds on which the chaotic attractors are built, we may expect that, working in the subspace (X, Y, Z), a sufficiently good topological characterization could be achieved. This seems to be supported by the comparison of figures 7 and 8, where one plane projection (figure 7) comes from a 4D space while the other (figure 8) comes from a 3D space.

A first-return map to a Poincaré section is then computed. It exhibits three monotonic branches separated by two critical points X_1 and X_2 (figure 9). The presence of three branches indicates that, in this example, the chaos is slightly more developed than for the original attractor since a few periodic orbits are then encoded with a symbol 2 [30]. We

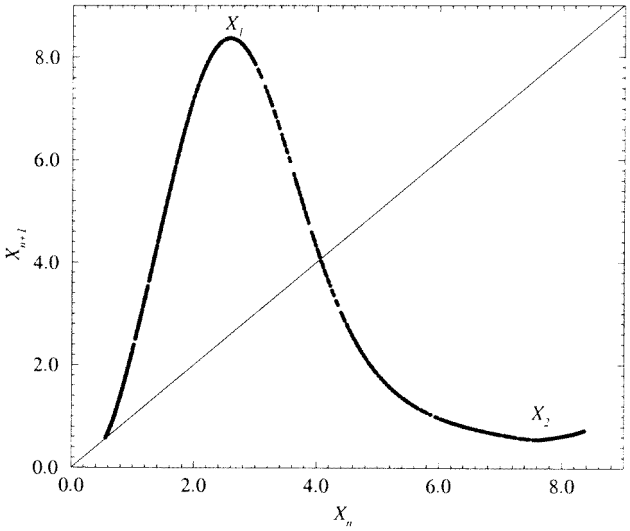

Figure 9. First-return map to a Poincaré section from the four-variable reconstructed model.

Table 2. Linking numbers of pairs of periodic orbits extracted from the reconstructed attractor. x designates couples of periodic orbits for which linking numbers cannot be counted in a plane projection due to the presence of long segments close to tangency.

	(1)	(10)	(100)	(101)	(1000)	(1001)
(10)	+1					
(100)	+1	+2				
(101)	+1	+2	+3			
(1000)	+1	+2	+3	+3		
(1001)	+1	+2	+3	*x*	+4	
(10000)	+1	+2	+3	+3	+4	+4
(10001)	+1	+2	+3	+3	*x*	*x*

therefore start by checking that the topological properties of the 4D reconstructed model are well characterized by a template with a linking matrix:

$$M \equiv \begin{bmatrix} 0 & -1 & -1 \\ -1 & -1 & -2 \\ -1 & -2 & -2 \end{bmatrix} \tag{19}$$

which is the linking matrix for a three-strip template of the Rössler system [30]. All linking numbers between pairs of periodic orbits extracted from the attractor generated by the reconstructed 4D model are then indeed found well predicted by this template as reported in table 2. The reconstructed attractor therefore presents topological properties compatible with the original Rössler system.

It remains to explain why the periodic orbits are more numerous than for the original Rössler system. It has been shown that noise benefits chaotic behaviour [25, 11] and, consequently, increases the population of periodic orbits. Since many segments of a chaotic trajectory are close to tangency in the reconstructed phase space spanned by the coordinates derived from the variable z of the Rössler system, discretization of the time series during the recording process acts like a noise contamination by diffusing the structure of the dynamics

in the region where tangencies are observed. The population of periodic orbits is therefore increased due to the measurement function. These perturbations are only located in a small region of the phase portrait rather than spread on the whole phase space and, therefore, are not efficiently smoothed by the reconstruction algorithm in contrast to what happens for a genuine noise contamination [11].

The increase of the population of periodic orbits is equivalent to a shift of the control parameter. Indeed, the kneading sequence for the 4D reconstructed dynamics is encoded by (20010) which is the one that we could obtain in the 3D original system for $a \approx 0.44$, in contrast with the actual value $a = 0.398$.

5. Conclusion

Many chaoticians understand Takens' theorem as stating that all variables of a dynamical system are equally effective in reconstructing the original dynamics from a scalar time series. Unfortunately, as demonstrated in the case of the Rössler system, different variables contain 'different levels of dynamical information'. In practice, this means that it could be easier to reconstruct the phase space from a particular variable or, conversely, it could be extremely difficult to reconstruct it from certain observables. Such lack of equivalence has been exemplified by using an observability index computed from the Jacobian matrix for the Rössler and Lorenz systems and the results are in good accord with previous findings. Although the concepts discussed in this paper are of great relevance in phase-space reconstruction and identification problems, as it stands it is limited to the case in which the Jacobian matrix is known *a priori*. Indeed, when we are facing an unknown system whose scalar time series only is known, the important problem is to know if it is a good observable or not. Currently, there is no answer to this question while the time evolution of a single variable is recorded. Nonetheless it is argued that it should be possible to reconstruct multivariable models and therefore Jacobians using the theory in section 3. This is left for future research.

Acknowledgments

LAA greatfully acknowledges financial support by CAPES, CNPq, FAPEMIG and PRPq/UFMG.

References

[1] Packard N H, Crutchfield J P, Farmer J D and Shaw R S 1980 Geometry from a time series *Phys. Rev. Lett.* **45** 712–16

[2] Broomhead D S and King G P 1986 Extracting qualitative dynamics from experimental data *Physica* **20D** 217–36

[3] Gibson J F, Farmer J D, Casdagli M and Eubank S 1992 An analytic approach to practical state space reconstruction *Physica* **57D** 1–30

[4] Agarwal A K, Ahalpara D P, Kaw P K, Prablakera H R and Sen A 1990 Model equations from a chaotic time series *J. Phys.* **35** 287–301

[5] Gouesbet G and Maquet J 1992 Construction of phenomenological models from numerical scalar time series *Physica* **58D** 202–15

[6] Baake E, Baake M, Bock H G and Briggs K M 1992 Fitting ordinary differential equations to chaotic data *Phys. Rev.* E **45** 5524–9

[7] Brown R, Rul'kov N F and Tracy E R 1994 Modeling and synchronizing chaotic systems from time-series data *Phys. Rev.* E **49** 3784–800

[8] Gouesbet G and Letellier C 1994 Global vector field reconstruction by using a multivariate polynomial L_2-approximation on nets *Phys. Rev.* E **49** 4955–72
[9] Judd K and Mees A 1995 On selecting models for nonlinear time series *Physica* **82D** 426–44
[10] Aguirre L A and Billings S A 1995 Dynamical effects of overparametrization in nonlinear models *Physica* **80D** 26–40
[11] Letellier C, Le Sceller L, Dutertre P, Gouesbet G, Fei Z and Hudson J L 1995 Topological characterization and global vector field reconstruction from an experimental electrochemical system *J. Phys. Chem.* **99** 7016–27
[12] Tufillaro N B, Wyckoff P, Brown R, Schreiber T and Molteno T 1995 Topological time series analysis of a string experiment and its synchronized model *Phys. Rev.* E **51** 164–74
[13] Takens F 1981 Detecting strange attractors in turbulence *Dynamical Systems and Turbulence, Warwick 1980 (Lecture Notes in Mathematics)* vol 898, ed D A R and L S Young (New York: Springer) pp 366–81
[14] Sauer T, Yorke J and Casdagli M 1991 Embeddology *J. Stat. Phys.* **65** 579–616
[15] Abarbanel H D I and Kennel M B 1993 Local false nearest neighbours and dynamical dimensions from observed chaotic data *Phys. Rev.* E **47** 3057–68
[16] Abarbanel H D I, Brown R, Sidorowich J J and Tsimring L Sh 1993 The analysis of observed chaotic data in physical systems *Rev. Mod. Phys.* **65** 1331–8
[17] Cao L 1997 Practical method for determing the minimum embedding dimension of a scalar time series *Physica* **110D** 43–52
[18] King G P and Stewart I 1992 Phase space reconstruction for symmetric dynamical systems *Physica* **58D** 216–28
[19] Letellier C and Gouesbet G 1996 Topological characterization of reconstructed attractors modding out symmetries *J. Physique* II **6** 1615–38
[20] Kugiumtzis D 1996 State space reconstruction parameters in the analysis of chaotic time series—the role of the time window length *Physica* **95D** 13–28
[21] Letellier C, Ringuet E, Maheu B, Maquet J and Gouesbet G 1997 Global vector field reconstruction of chaotic attractors from one unstable periodic orbit *Entropie* **202/203** 147–53
[22] Le Sceller L, Letellier C and Gouesbet G 1996 Global vector field reconstruction taking into account a control parameter evolution *Phys. Lett.* A **211** 211–16
[23] Gershenfeld N 1988 An experimentalist's introduction to the observation of dynamical systems *Directions in Chaos* vol 2, ed Hao Bai Lin (Singapore: World Scientific) pp 310–84
[24] Demazure M 1989 *Catastrophes et Bifurcations* (Paris: Ellipse)
[25] Letellier C 1994 Caractérisation topologique et reconstruction d'attracteurs étranges *PhD Dissertation* Université de Paris VII
[26] Rice J R 1964 *The approximation of functions* vol 1 (Reading, MA: Addison-Wesley)
Rice J R 1969 *The approximation of functions* vol 2 (Reading, MA: Addison-Wesley)
[27] Aguirre L A 1995 Controllability and observability of linear systems: some noninvariant aspects *IEEE Trans. Educ.* **38** 33–9
[28] Kailath T 1980 *Linear Systems* (Englewood Cliffs, NJ: Prentice Hall)
[29] Mindlin G B, Solari H G, Natiello M A, Gilmore R and Hou X J 1991 Topological analysis of chaotic time series data from the Belousov–Zhabotinski reaction *J. Nonlinear Sci.* **1** 147–73
[30] Letellier C, Dutertre P and Maheu B 1995 Unstable periodic orbits and templates of the Rössler system: toward a systematic topological characterization *Chaos* **5** 271–82